ELSEVIER

Surface Science 395 (1998) 248–259

surface science

Adsorption of methanol, ethanol and water on well-characterized Pt–Sn surface alloys

Chameli Panja, Najat Saliba, Bruce E. Koel *

University of Southern California, Department of Chemistry, Los Angeles, CA 90089-0482, USA

Received 18 March 1997; accepted for publication 15 July 1997

Abstract

Adsorption and desorption of methanol (CH_3OH), ethanol (C_2H_5OH) and water on Pt(111) and two, ordered, Pt–Sn alloys has been studied primarily using temperature-programmed desorption (TPD) mass spectroscopy. The two alloys studied were the $p(2\times2)$Sn/Pt(111) and $(\sqrt{3}\times\sqrt{3})R30^\circ$ Sn/Pt(111) surface alloys prepared by vapor deposition of Sn on Pt(111), with $\theta_{Sn}=0.25$ and 0.33, respectively. All three molecules are weakly bonded and reversibly adsorbed under UHV conditions on all three surfaces, molecularly desorbing during TPD without any decomposition. The two Pt–Sn surface alloys were found to chemisorb both methanol and ethanol slightly more weakly than on the Pt(111) surface. The desorption activation energies measured by TPD, and hence the adsorption energies, of both methanol and ethanol progressively decrease as the surface concentration of Sn increases, compared with Pt(111). The decreased binding energy leads one to expect a lower reactivity for these alcohols on the two alloys. The sticking coefficients and the monolayer coverages of these alcohols on the two alloys were identical to that on Pt(111) at 100 K, independent of the amount of Sn present in the surface layer. Alloying Sn in Pt(111) also slightly weakens the adsorption energy of water. Water clusters are formed even at low coverages on all three surfaces, eventually forming a water bilayer prior to the formation of a condensed ice phase. These results are relevant to a molecular-level explanation for the reactivity of Sn-promoted Pt surfaces that have been used in the electro-oxidation of simple organic molecules. © 1998 Elsevier Science B.V.

Keywords: Adsorption energy; Ethanol; Methanol; Pt–Sn alloys; Sicking coefficient; Temperature programmed desorption; Water

1. Introduction

The use of simple organic molecules such as methanol, ethanol, formic acid and formaldehyde as future electrochemical fuels has several advantages. In addition to their high energy density [1], they are relatively nontoxic and easy to store and handle. Advanced fuel cells using methanol are already being developed [2]. Crucial to the operation of these electrochemical systems is the interaction of the fuel with the electrode surface.

The oxidation of methanol on different metal catalysts has been studied [3–8]. The principle limitation in using an electrode (electrocatalyst) with a viable organic fuel is the poisoning of the electrode by some intermediate and/or product produced by the reaction. Identified poisons are adsorbed hydrogen (H_{ads}), formyl species (CHO_{ads}) and carbon monoxide (CO_{ads}) [9,10]. The most active catalysts for methanol oxidation are defined as those having a low surface concentration of all poisoning species. These are either platinum catalysts promoted by electrodeposition of certain metals [11] or alloys of platinum such as Pt–Ru [12–14] or Pt–Sn [13–19]. For the Pt–Sn

* Corresponding author. Fax: (+1) 213 740.3972; e-mail: koel@cheml.usc.edu

0039-6028/98/$19.00 © 1998 Elsevier Science B.V. All rights reserved.
PII S0039-6028(97)00629-8

systems, there are controversies about the state of Sn in these catalysts and the activity of such electrodes. Most reports [13,15–17] state that Pt–Sn appears to be the most active catalyst in a sulfuric acid solution at a temperature above 40°C. In contrast, others report either an inhibition or an activity comparable to that of pure Pt [14,18,19]. Haner et al. [18] studied the electro-oxidation of methanol on Pt–Sn alloys and found no Pt–Sn alloy of any composition that was more active than pure platinum. While the use of ethanol in a fuel cell has been considered [20,21], the oxidation of ethanol on different metal electrodes is much less studied and ethanol is still of primarily academic interest due to the addition of one carbon atom that implies more intermediates that could possibly poison the electrode surface.

Surface science studies in ultra-high vacuum (UHV) of methanol and ethanol adsorption on metal surfaces such as Pd(111), Pt(111) and Pt(110) have been carried out [22–24]. Methanol decomposes on Pd(111) to form CO and H_2, while ethanol undergoes C–C bond cleavage to form CO, H_2 and methane (CH_4) [22]. Methanol and ethanol weakly and reversibly adsorb and desorb molecularly from Pt(111) [25,26]. Indeed, the first four (C_1–C_4) alcohols all have low heats of adsorption (11–15 kcal/mole) on Pt(111) [25]. The small amount of decomposition (10%) into CO, H_2 and C_{ads}, in early reports concerning adsorbed alcohols on Pt(111) was eventually shown by Dubois et al. [26] to be due to defect sites present at the surface. An outstanding question is whether or not the presence of Sn in the surface layer of Pt–Sn alloys will alter the chemistry of methanol and ethanol on the surface.

The interaction of water with transition metal surfaces is also an important topic for discussion of the electrode chemistry in electro-oxidation of alcohols. Because water–metal interactions are so ubiquitous for practical and fundamental considerations in many disciplines including corrosion, electrochemistry and catalysis, the adsorption of water on transition metals has been extensively investigated in the past and the platinum surface has been of special interest in heterogeneous catalysis and electrochemistry. An excellent review of water adsorption has been given by Thiel and Madey [27]. Even at the lowest coverages, water desorbs in two peaks, 196 and 178 K, and at higher coverages, there are three distinct physisorbed peaks, 160–167; 170–171; and 177–180 K, ascribed to multilayer ice, a bilayer region and a nonbilayer region, respectively [28,29]. Hydrogen-bonded clusters are present even at very low coverages. From photoelectron [30] and vibrational spectra [31,32], it was concluded that the "monolayer" consists of a two-tiered, three-dimensional structure, called the bilayer. The structure of the bilayer is such that the bottom half of the water molecules are directly bonded to the surface through the oxygen atoms and the top half of the water molecules are held in the structure by two or three hydrogen bonds to the lower molecules. The high-temperature, "chemisorbed" state of water corresponding to the desorption peak at 185–196 K on Pt(111) surfaces has been assigned to a surface recombination reaction of coadsorbed hydroxyls that are formed at defects or from dissociation induced by preadsorbed oxygen (from the background) [28,29].

In order to aid discussion and resolution of the controversies discussed above and to provide a firm foundation for understanding the chemistry relevant to electro-oxidation of alcohols over Sn-promoted Pt electrodes, it is important to define the interactions of simple alcohols with well-defined Pt–Sn alloy surfaces. In our present study, we have investigated the interaction of methanol, ethanol and water with Pt–Sn surfaces under UHV conditions by temperature-programmed desorption (TPD). The objective of this study was to determine the adsorption energies of these molecules on Pt(111) and two different bimetallic surfaces, the (2×2) and $(\sqrt{3}\times\sqrt{3})R30^\circ$ Sn/Pt(111) surface alloys. Specifically, we wanted to evaluate whether the presence of Sn in the surface layer leads to an increase in adsorption energy or thermally activates these molecules for reaction due to the thermodynamic driving force provided by the Sn–O interaction.

2. Experimental methods

The experiments were conducted in an ion-pumped stainless-steel vacuum chamber (base

pressure 1×10^{-10} Torr) equipped with low-energy electron diffraction (LEED), Auger electron spectroscopy (AES) using a double-pass cylindrical mirror analyzer, a shielded UTI 100C quadrupole mass spectrometer (QMS) for temperature-programmed desorption (TPD), an ion gun for sputtering, and gas and metal dosing facilities.

The Pt(111) crystal could be heated resistively to 1100 K or cooled to 90 K using liquid nitrogen. A chromel–alumel thermocouple was spot welded to the crystal to monitor the temperature. The crystal was cleaned by repeated cycles of Ar^+ ion bombardment, annealing in vacuum at 1100 K and heating in 5×10^{-8} Torr O_2 at 800 K. The cleanliness and long-range order of all surfaces were checked using AES and LEED prior to each experiment.

Methanol (Mallinckrodt Chemical, 99.9%), ethanol (Quantum Chemical Corporation, 99.9%) and deionized water were placed in glass reservoirs attached to a stainless-steel dosing line and used as supplied after degassing by multiple freeze–pump–thaw cycles. These gases were exposed on the Pt crystal by a microcapillary array doser connected to the gas line through a leak valve. For water, some background dosing was also used for small exposures in addition to microcapillary dosing. All the exposures listed in this paper are given simply in terms of the dosing time for a fixed dosing pressure (about 4×10^{-10} Torr in the background); no attempt has been made to correct for flux enhancement of the doser or ion gage sensitivity. The mass spectrometer in the chamber was used to check the purity of the gases during dosing. For all of the TPD experiments, the heating rate was ~ 4 K/s.

The (2×2) Sn/Pt(111) and $(\sqrt{3} \times \sqrt{3})R30^\circ$ Sn/Pt(111) surface alloys were prepared by evaporating several monolayers of Sn onto the Pt(111) crystal surface and subsequently annealing the sample to 1000 K for 10 s. Depending on the initial deposited Sn coverage, the annealed surface exhibits either a (2×2) or a $(\sqrt{3} \times \sqrt{3})R30^\circ$ Sn/Pt(111) structure, as observed by LEED [33]. These LEED patterns for the surfaces prepared as above are due to substitutional surface alloys with $\theta_{Sn} = 0.25$, corresponding to the (111) face of Pt_3Sn, and $\theta_{Sn} = 0.33$, corresponding to a Pt_2Sn surface, in which the Sn atoms protrude 0.02 nm above the surface Pt plane [34]. For the (2×2) structure, three-fold Pt sites are present, but none of these are adjacent three-fold Pt sites. All three-fold sites comprised of only Pt are eliminated for the $\sqrt{3}$ structure and the distance between adjacent two-fold sites is increased. For brevity throughout this paper, we will refer to the $p(2 \times 2)$Sn/Pt(111) and $(\sqrt{3} \times \sqrt{3})R30^\circ$ Sn/Pt(111) surface alloys as the (2×2) and $\sqrt{3}$ alloy surfaces, respectively.

3. Results and discussion

3.1. Methanol and ethanol adsorption

A series of TPD spectra for methanol (CH_3OH) desorption from Pt(111) and the (2×2) and $\sqrt{3}$ alloys are shown in Figs. 1–3, respectively. All methanol exposures were given with the surface temperature at 95–100 K. In each case, a clear separation occurs between a high-temperature peak due to a chemisorbed state and a low-temperature peak arising from desorption from a condensed, physisorbed layer. With increasing coverage in the monolayer, a small shift to lower temperatures is seen for the chemisorption peak. The multilayer, or condensed phase, peak formed at larger exposures occurs at 145 K for all three surfaces. On Pt(111) at relatively low exposures, a desorption peak at 194 K is observed from the monolayer and this peak shifts only slightly to a lower temperature (183 K) at saturation coverage of the monolayer, presumably due to lateral interactions between methanol molecules. Alloying Pt with Sn lowers the desorption temperature for low coverages of methanol in the monolayer from 194 K on Pt(111) to 186 and 179 K on the (2×2) and $\sqrt{3}$ alloy surfaces, respectively. At saturation coverage in the monolayer, the desorption peak is reduced from 183 K on Pt(111) to 177 and 170 K on (2×2) and $\sqrt{3}$ alloy surfaces, respectively. Because of the very small shifts in the TPD peak maxima with increasing methanol coverage for these three surfaces, we have attributed first-order

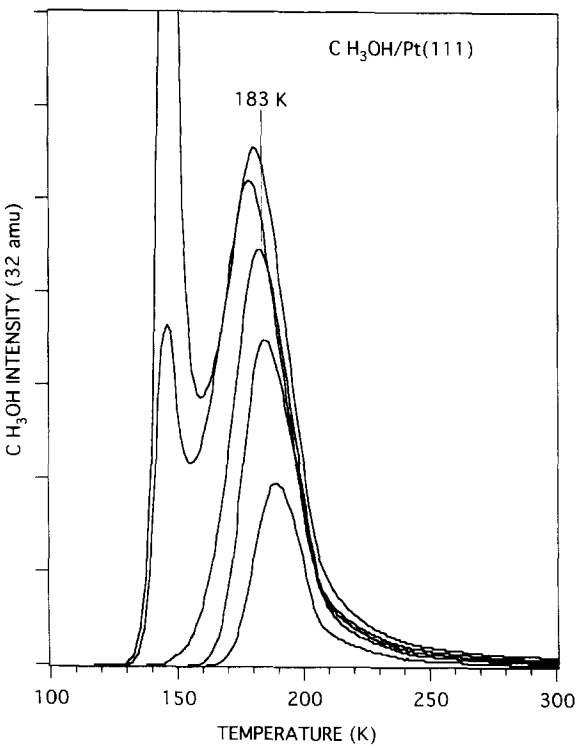

Fig. 1. Methanol TPD spectra after methanol exposures on the Pt(111) surface. The multilayer desorption peak at the highest exposure has been cut off. Exposures from the bottom to top are 10, 20, 40, 60 and 70 s.

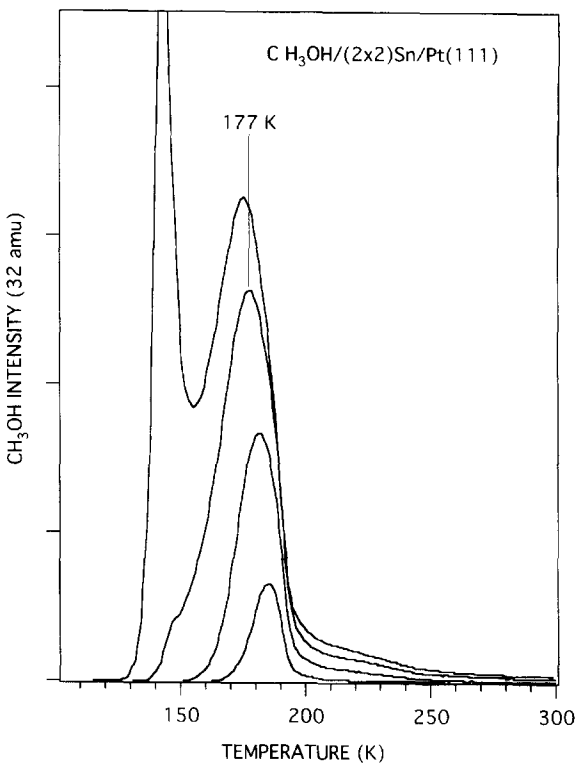

Fig. 2. TPD spectra of methanol on the (2×2) Sn/Pt(111) surface at different coverages. The exposures from the bottom to top are 5, 20, 40 and 60 s.

kinetics to the methanol desorption from all of these surfaces.

Evidence for CO and H_2 evolution from methanol decomposition was monitored during TPD from all three surfaces following methanol exposure. No appreciable CO or H_2 desorption was detected. Estimation of the maximum amount of decomposition using these CO and H_2 peak areas yield, in each case, decomposition amounts of $<5\%$, and we attribute this to contributions from defect sites and coadsorption of impurities from the background gases. Consistent with these TPD results, no carbon or oxygen was detected by AES following TPD.

In Figs. 4–6, we show a series of TPD spectra for ethanol (C_2H_5OH) desorption following ethanol dosing on Pt(111) and the (2×2) and $\sqrt{3}$ alloy surfaces, respectively, at 95–100 K. These TPD spectra are quite analogous to those for methanol desorption, except that the desorption temperature of ethanol is higher than methanol on all the three surfaces at all coverages due to the higher molecular weight and larger size of ethanol which leads to stronger adsorption and larger condensation energies on the surface. In each case, a distinct monolayer desorption peak can be observed and this peak shifts slightly to lower temperatures with increasing coverage in the monolayer. The ethanol multilayer formed for larger exposures has a desorption peak temperature of 155 K from all the three surfaces for nearly identical exposures. On Pt(111), the desorption peak maximum for a low coverage of ethanol in the monolayer occurs at 213 K, but shifts to 202 K at saturation coverage in the monolayer due to lateral interactions. The desorption peak temperature of ethanol in the monolayer progressively decreases with increasing Sn concentration in the surface alloy. At relatively low ethanol coverages,

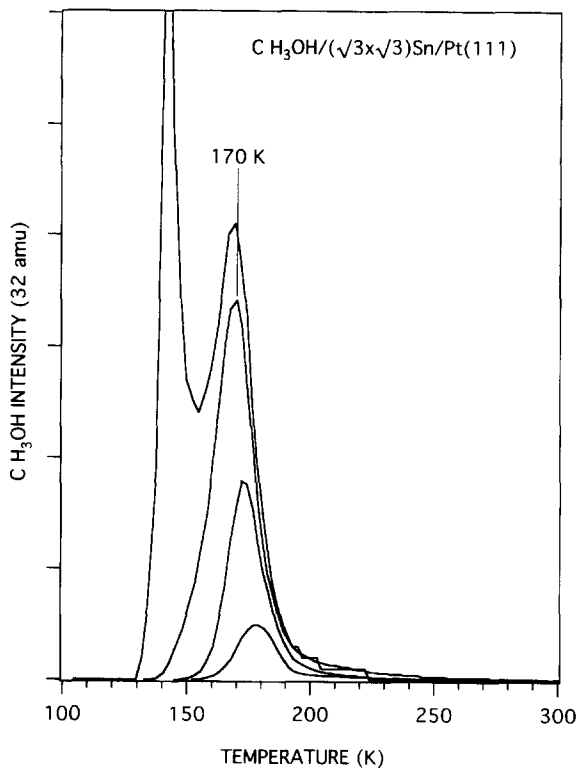

Fig. 3. Methanol TPD spectra after methanol exposures on the $(\sqrt{3}\times\sqrt{3})$R30° Sn/Pt(111) surface with exposures from bottom to top of 10, 20, 40 and 60 s.

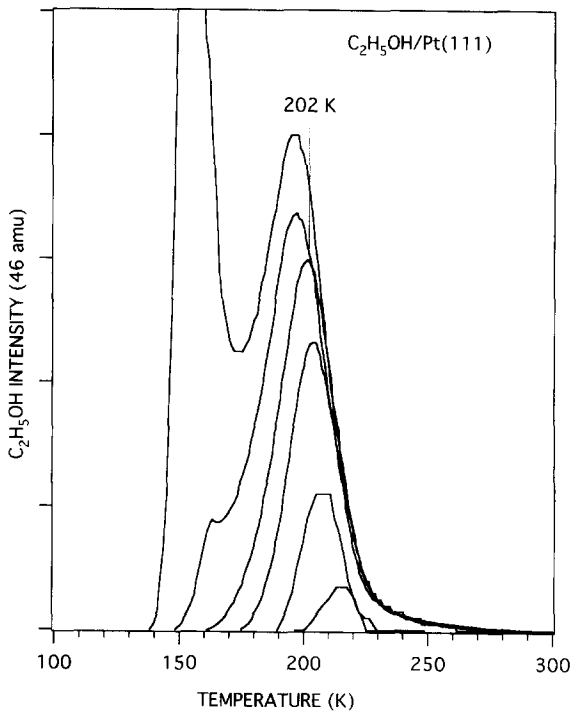

Fig. 4. Ethanol TPD spectra after ethanol exposures on the Pt(111) surface at different coverages. The exposures from bottom to top are 5, 10, 20, 40, 60 and 80 s.

desorption occurs in peaks at 213, 206 and 197 K on Pt(111) and the (2×2) and $\sqrt{3}$ alloy surfaces, respectively, and peaks occur at 202, 200 and 190 K for monolayer saturation coverages on these three surfaces, respectively. The appearance of the ethanol TPD spectra on all the three surfaces also suggests first order desorption kinetics.

The adsorption–desorption behavior of ethanol was found to be entirely reversible with no evidence of decomposition, even though ethanol is expected to have a higher reactivity than methanol due to the presence of β-hydrogen atoms. Uptake curves showing the adsorption kinetics and relative saturation coverages for methanol and ethanol chemisorbed on the three surfaces are shown in Fig. 7a and b, respectively. The slopes of these uptake curves are proportional to the sticking coefficients, S, of these molecules on these surfaces. First, we find that $S=1$ for the population of the chemisorbed state on these surfaces at 100 K by comparison with the uptake into the condensed multilayers at higher coverages (not shown) and the knowledge that $S=1$ for the condensation of many hydrocarbons [35] and water [29]. Second, we find that the value of the initial sticking coefficient at "zero" coverage, S_0, is maintained throughout population of the monolayer, i.e., constant sticking coefficient, for adsorption on these surfaces at 100 K. *We find that the value of S_0 (and S) is not affected by the presence of Sn in the surface layer.* Thus, alloyed Sn does not effectively decrease the adsorption rate constant of these two alcohols on Pt–Sn alloys compared with the Pt(111) surface up to $\theta_{Sn}=0.33$. Even if Sn is not directly involved in the bonding of these molecules, this would be consistent with the important influence of a precursor state present at the Sn sites, which we have previously discussed as the modifier precursor state [36]. These curves also show that the same monolayer coverage is obtained for methanol and

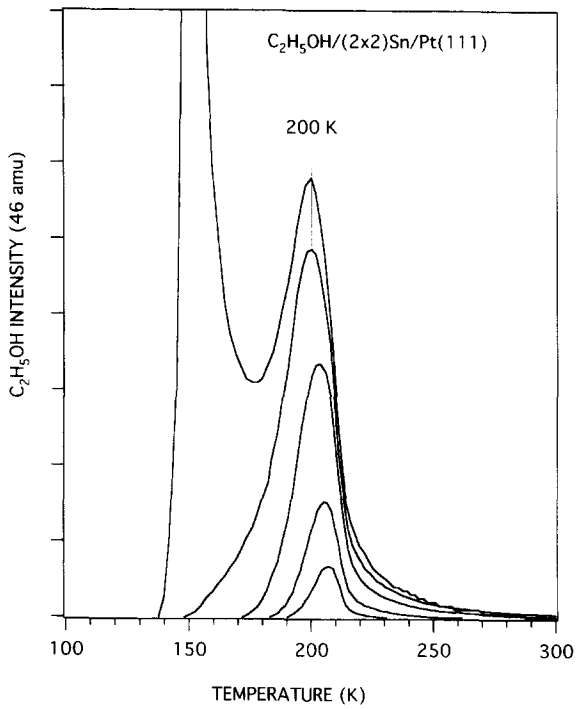

Fig. 5. TPD spectra of ethanol on the (2 × 2) Sn/Pt(111) surface with different coverages. The exposures from bottom to top are 10, 20, 40, 60 and 120 s.

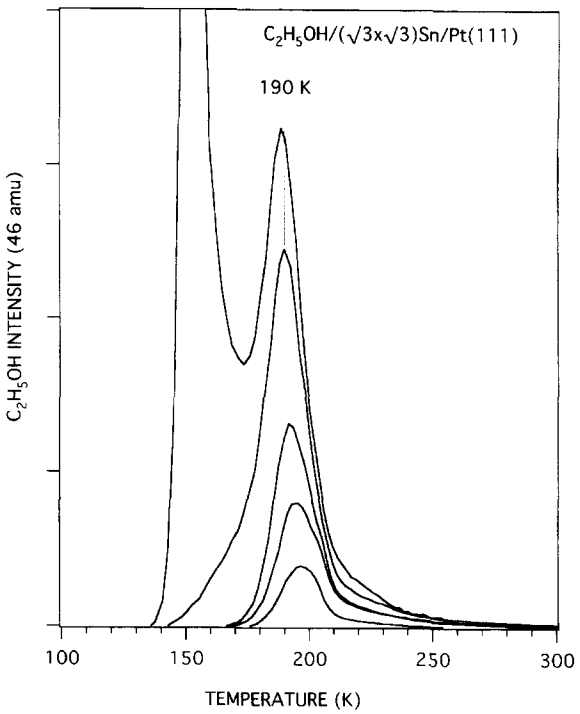

Fig. 6. Ethanol TPD spectra after ethanol exposures on the $(\sqrt{3} \times \sqrt{3})R30^{\circ}$ Sn/Pt(111) surface. The exposures from bottom to top are 5, 10, 20, 40 and 80 s.

ethanol chemisorbed on the two Pt–Sn surface alloys compared with that on Pt(111). *We find that the chemisorbed methanol and ethanol monolayer coverages on Pt(111) and the (2 × 2) and* $\sqrt{3}$ *surface alloys are independent of the alloyed Sn concentrations in these three surfaces.* Thus, alloyed Sn does not effectively inhibit access to the surface for the adsorption of these two alcohols on Pt–Sn alloys compared to the Pt(111) surface up to $\theta_{Sn} = 0.33$. This suggests that there is only a small ensemble of a few Pt atoms required for chemisorption.

A comparison of the desorption peaks in TPD for relatively low initial surface coverages of about 10% of a saturation monolayer coverage (to minimize lateral interactions) of methanol and ethanol on Pt(111) and the (2 × 2) and $\sqrt{3}$ alloy surfaces is shown in Fig. 8. These spectra show clearly the influence of alloyed, surface Sn in reducing the desorption temperatures to progressively lower values as the surface concentration of Sn increases in the surface alloy. A decrease in peak temperature indicates slightly weaker adsorbate–surface bonding and this effect can be quantified to give desorption activation energies in several ways. The simplest method is an analysis of the desorption peak maxima using Redhead [37] analysis, assuming a pre-exponential factor of 10^{13}/s and first-order kinetics. These results are given in Table 1. A method that does not require an assumption of the pre-exponential factor or kinetic order and is often more accurate is derived from making an Arrhenius plot from the desorption rate curves. This is also sometimes referred to as leading-edge analysis [38,39]. These Arrhenius plots of ln(rate) versus $1/T$, where the desorption rate is proportional to the TPD peak intensity, gave curves that were excellently described by straight lines for temperatures below the peak maximum. The slopes (slope $= E_a/R$) of these lines give the desorption activation energies for methanol and ethanol on the three surfaces and these are reported in

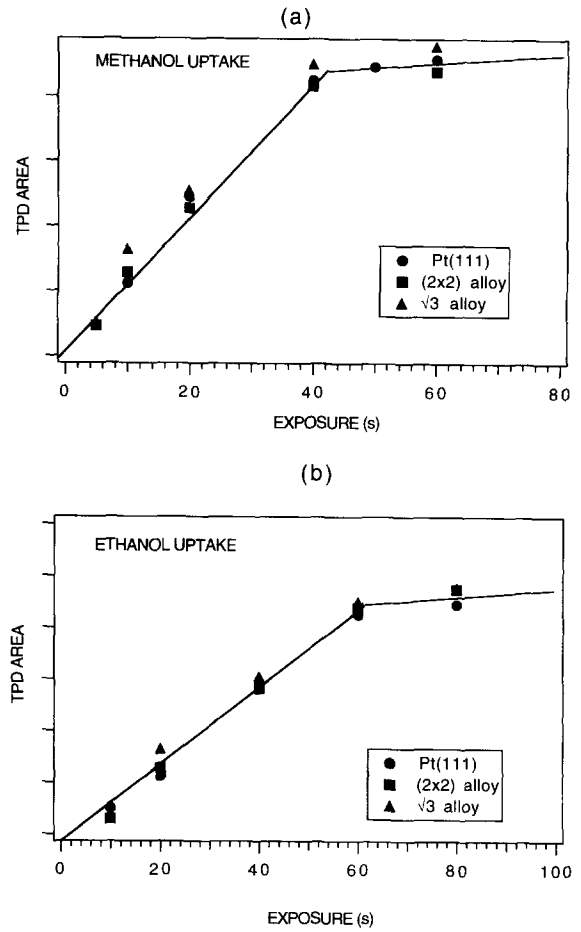

Fig. 7. (a) Methanol and (b) ethanol uptake curve results from TPD experiments for different exposures on the Pt(111), (2 × 2) and $\sqrt{3}$ alloy surfaces.

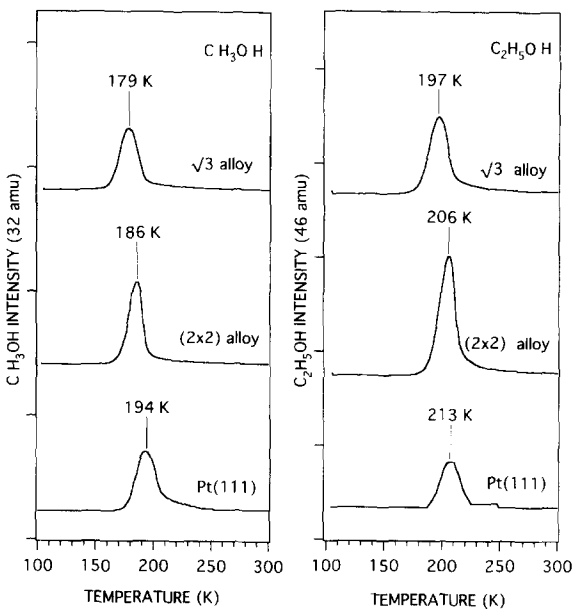

Fig. 8. Comparison of methanol and ethanol desorption spectra for $\theta \cong 0.1\theta_{sat}$ of methanol and ethanol on the Pt(111), (2 × 2) and $\sqrt{3}$ surface alloys.

Table 1
Thermal desorption peak temperatures (top entries, in K) and desorption activation energies in kJ/mol (bottom entries) for methanol, ethanol and water obtained at about 10% of the monolayer saturation coverages on Pt(111) and two Pt–Sn surface alloys. The left-hand values given in parentheses are activation energies obtained by Redhead analysis; the right-hand values were determined by leading-edge analysis

Molecule	Pt(111)	(2 × 2)	$\sqrt{3}$
Methanol	194	186	179
	(49, 47)	(47, 44)	(45, 41)
Ethanol	213	206	197
	(54, 51)	(52, 53)	(50, 47)
Water (bilayer)	162	156	152
	(41, 43)	(39, 43)	(38, 44)

Table 1. The Redhead method and the Arrhenius plots give consistent results within ±6 kJ/mole Since the molecular adsorption of these alcohols is not activated on these surfaces, the desorption energy is equal to the adsorption energy. The presence of alloyed Sn in Pt–Sn surfaces does not have a large effect on the methanol and ethanol heats of adsorption, but does slightly decrease the adsorption energy of methanol and ethanol on these surfaces in comparison to Pt(111).

To summarize methanol and ethanol interactions on Pt–Sn alloys, alloyed Sn does not have a large influence on Pt(111) chemistry. We note that ultraviolet photoelectron spectroscopy (UPS) has shown that alloying causes only small changes in the Pt d-DOS and in particular the DOS near E_F [40]. However, because of the stronger Sn–O bond compared with the Pt–O bond and the thermodynamic driving force for forming tin oxide, it is possible that Sn would increase the reactivity of the clean Pt(111) surface, either increasing the adsorption energies of alcohols or lowering the activation barrier to dissociative adsorption. This intuitive idea does not correctly predict our results.

We observed a decrease in the adsorption energies because Sn is not directly involved in the bonding of these molecules to the surface and the subtle localization of charge due to Pt–Sn bonding weakens the adsorbate–surface interaction. Our values for the adsorption energetics should be quite useful in calculating surface coverages and residence times under a variety of conditions other than those of UHV. The intuitively expected increase in alcohol reactivity due to Sn was also not observed. We know from our desorption measurements that the activation barriers to dissociate methanol or ethanol on these alloy surfaces certainly exceed 41–54 kJ/mol. It is reasonable to assume that the barriers to dissociation exceed those on Pt(111) since the adsorption energies are smaller. Our data are consistent with the more recent results for electro-oxidation of methanol [14,18,19] that show that Pt–Sn alloys are not more active than pure Pt.

3.2. *Water adsorption*

Fig. 9 shows the TPD spectra after H_2O was dosed on clean Pt(111) at 100 K. The inset shows additional spectra for very low exposures. Even for these very low exposures, two peaks appear, one near 185 K and a second at 163 K, similar to that observed previously [28,29]. The feature at 185 K is always small and saturates at relatively low exposures. This broad peak has been assigned to a surface recombination reaction of coadsorbed hydroxyls that are formed at defects or from dissociation induced by preadsorbed oxygen (from the background) [28,29]. The formation of the 163 K peak, which shifts to 167 K near saturation coverage, is attributed to water-island or cluster formation due to hydrogen bonding even at very low coverages because the energy associated with hydrogen bonding is comparable to the water–surface interaction. We did not resolve a second peak in the bilayer region as Jo et al. [29] observed; this is most likely to be due to a small amount ($\sim$5% ML) of preadsorbed hydrogen from background contamination on the Pt(111) surface [29]. Finally, another peak arises at 161 K which shifts to higher temperature with increasing exposure and does not saturate. One "monolayer" has been

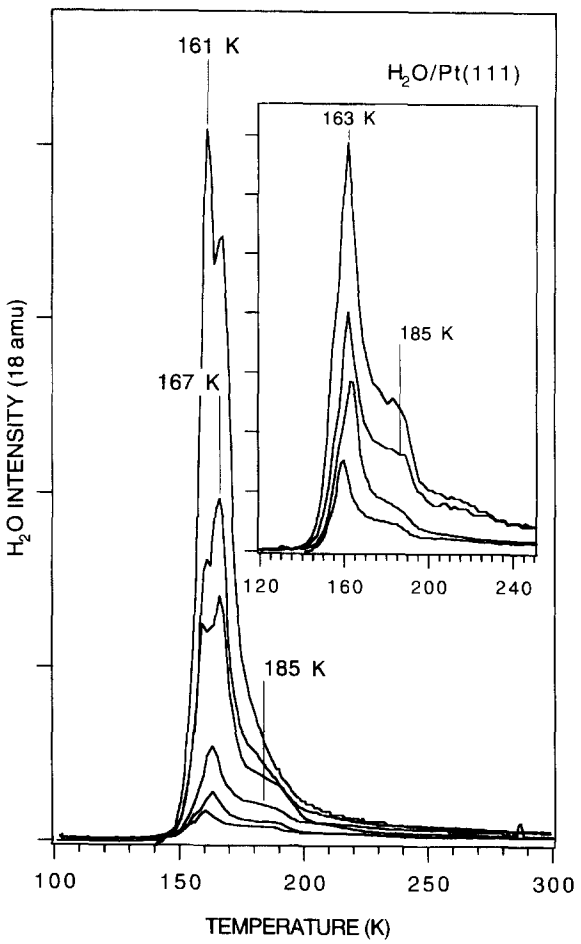

Fig. 9. TPD spectra of water dosed at 100 K on the Pt(111) surface with different exposures.

defined as the coverage corresponding to the highest exposure which did not give a 161 K desorption peak. This monolayer saturation coverage of water on Pt(111) corresponds to a bilayer with 0.67 H_2O molecules per Pt atom [27].

On both the (2×2) and $\sqrt{3}$ surface alloys, no high-temperature "chemisorption" peak was found, as shown in Fig. 10Fig. 11. Immediately at the lowest exposures, a H_2O TPD peak arises at about 156 K for the (2×2) alloy and at 152 K for the $\sqrt{3}$ alloy and shifts to higher temperatures (165–166 K) with increasing coverages. These peak shapes are appear like those for zero-order kinetics. First, alloying with Sn completely poisons the Pt(111) surface for the high-temperature "che-

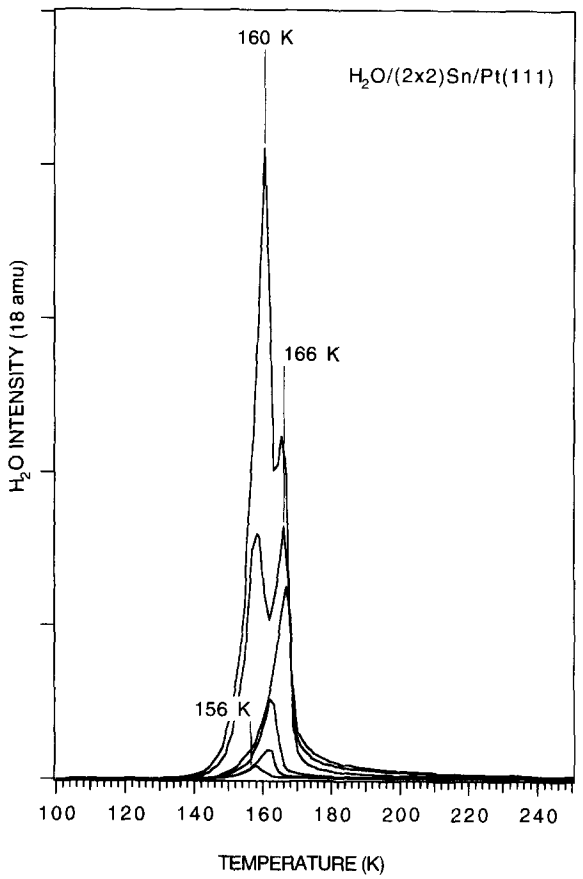

Fig. 10. Water TPD spectra after water exposures on the (2 × 2) Sn/Pt(111) surface alloy with different coverages.

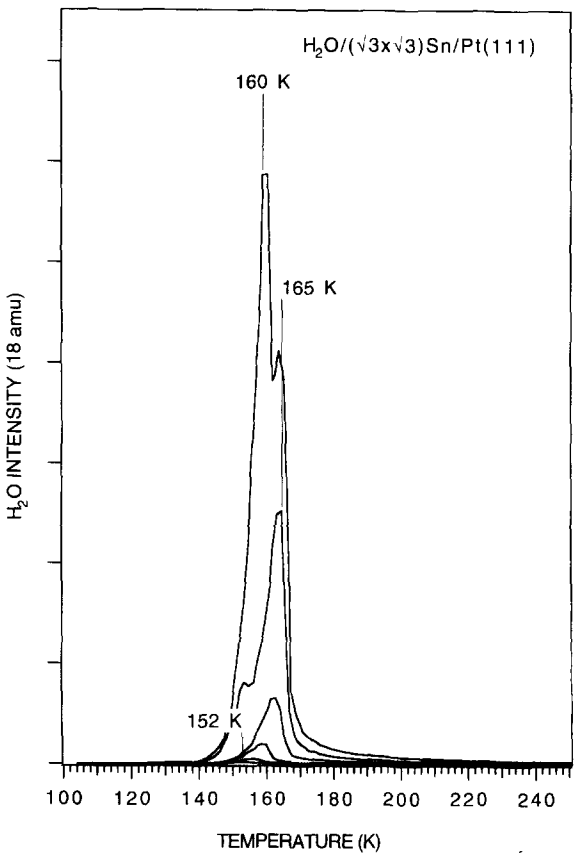

Fig. 11. TPD spectra of water on the $(\sqrt{3}\times\sqrt{3})R30^{\circ}$ Sn/Pt(111) surface with different coverages.

misorption" peak of water. This could be due to titration of defect sites by alloyed Sn and/or the fact that these Pt–Sn alloys do not dissociatively chemisorb O_2 [41]. Second, the peak that appears at 166–165 K for both of the alloyed surfaces is identical to that (167 K) for the Pt(111) surface and the overall behavior of this peak with increasing coverage is also nearly the same. This desorption peak is certainly due to island formation from hydrogen-bonded water clusters and, furthermore, we propose that this peak arises from the water bilayer on the alloy surfaces. A comparison of the areas of the 165–167 K peaks at saturation coverage in these states on all three surfaces gives the same values. Hence, the "monolayer" of water that forms on Pt(111) with a bilayer structure also forms on the two alloys and the kinetics and energetics of the desorption of this bilayer and subsequent multilayers is identical on all three surfaces. Evidently the presence of alloyed Sn in the surface layer of the Pt–Sn alloy has a similar effect to that observed for preadsorbed hydrogen or oxygen [29] on Pt(111) in that some orientation or ordering requirement cannot be satisfied on the alloy surface to cause the characteristic "two peak" desorption of the bilayer structure. (The preadsorption of contaminant hydrogen or oxygen can no longer be an explanation for the merging of these two peaks as on Pt(111) in Fig. 9 since the two alloys do not dissociatively adsorb H_2 or O_2 [41].)

In order to probe any subtle differences in the direct bonding interactions of water with these three surfaces, we show desorption spectra in

Fig. 12 for initial water coverages that are about 10% of the saturation monolayer coverage. The main TPD peak decreases from 163 K on Pt(111) to 156 K on the (2×2) alloy to 152 K on the $\sqrt{3}$ alloy. The results from the Arrhenius plots from a leading-edge analysis are summarized in Table 1 along with those obtained by using Redhead analysis. With increasing Sn concentration in the alloys, the bonding of water to the surface is reduced slightly. Regarding the reactivity of these surfaces, the activation barrier for dissociative adsorption of water exceeds 38–44 kJ/mol on these three surfaces.

Fig. 13 illustrates and compares the influence of increasing alloyed Sn concentration on the adsorption energetics of methanol, ethanol and water on Pt(111) and the (2×2) and $\sqrt{3}$ alloy surfaces. The molecular desorption peak temperatures are shown for desorption at relatively low coverages of about 10% of the monolayer saturation coverage in order to reduce the influence of lateral interactions in the adsorbed layer. In addition, the right-hand axis in Fig. 13 approximately indicates the corresponding desorption activation energies (this is an approximate guide since there is not strictly a linear relationship between the peak temperature and the activation energy). As we have discussed,

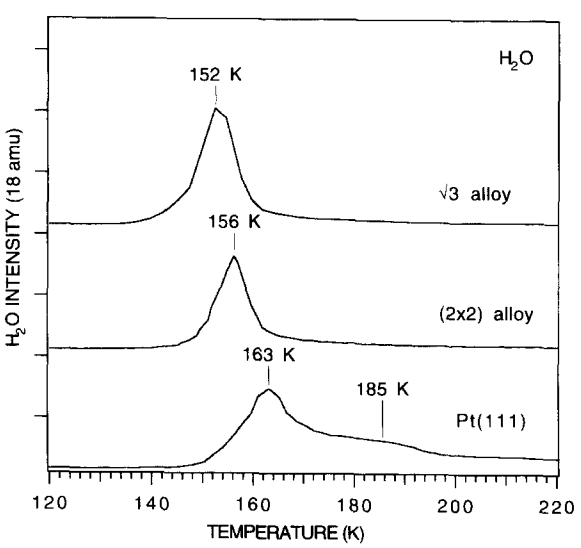

Fig. 12. Comparison of the desorption peak temperature of about 10% saturation monolayer coverage of water on the Pt(111), (2×2) and $\sqrt{3}$ alloy surfaces.

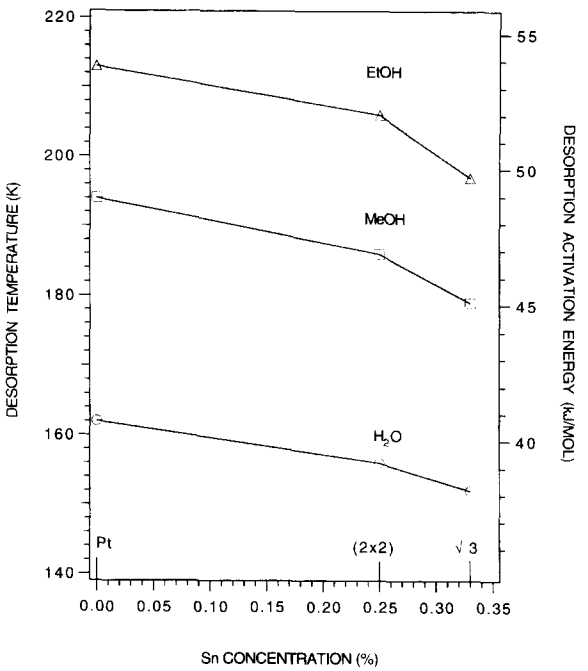

Fig. 13. Influence of the alloyed Sn concentration on the desorption peak temperature of methanol ethanol and water in the Sn/Pt surface alloys. The right-hand axis gives an estimation of the corresponding molecular desorption energies.

alloying Sn with Pt(111) causes a weak reduction in the adsorbate–surface bonding in all cases, presumably due to increased localization of Pt orbitals resulting from Pt–Sn bonding interactions. The decrease in the desorption temperature is not linear with an increase in the surface Sn concentration for any of the three molecules studied, the decrease in adsorption energy being relatively larger for the $\sqrt{3}$ alloy than the (2×2) alloy for all of the molecules. We have observed a similar behavior for several alkenes [42] on these alloys and we interpreted this as due to the absence of pure-Pt three-fold sites on the $\sqrt{3}$ alloy and the importance of these sites in chemisorption bonding. Because these molecules are so weakly bonded to the surfaces, such a connection here is more tenuous. The smaller influence of alloying on the bonding of water on the (2×2) and $\sqrt{3}$ alloys is justifiable due to the relatively smaller role played by the substrate surface in the adsorption energy because of the much larger importance of hydrogen

bonding in the water overlayer compared to that for methanol and ethanol.

4. Summary

Methanol and ethanol molecularly desorb from Pt(111) and the (2×2) and $(\sqrt{3}\times\sqrt{3})R30^\circ$ Sn/Pt(111) surface alloys without any decomposition under UHV conditions. Both alloy surfaces chemisorb these molecules slightly more weakly than the clean Pt(111) surface. The adsorption rate constant, i.e. the sticking coefficient, and the monolayer coverage of methanol and ethanol are uneffected by alloying Sn into the Pt surface. The latter observation suggests that an ensemble size of only a few Pt atoms is required for chemisorption. In addition, the activation barriers for the dissociation of methanol and ethanol exceed 41–54 kJ/mol on these Pt–Sn alloys and chemisorption of these alcohols does not oxidize the Sn in the alloy under UHV conditions.

Water is only weakly adsorbed on all three surfaces studied and a thermally stabilized bilayer structure is formed on the two alloy surfaces similarly to Pt(111). The desorption temperature and desorption activation energy of this bilayer and subsequent condensed layers are unaffected by alloying, even though there is evidence that at very low coverages there is a small weakening of the direct interaction of water molecules with the surface with increasing Sn concentration.

In general, for all three molecules, a trend is observed for a small decrease in the desorption activation energies with increasing Sn concentration in the series Pt(111), (2×2) alloy and $\sqrt{3}$ alloy surfaces, with a relatively larger influence upon forming the $\sqrt{3}$ alloy. This is consistent with recent results that show that Pt–Sn alloys are not more active than pure Pt for electro-oxidation of methanol [14,18,19]. Our data provide benchmarks for discussing the surface chemistry of alcohols on Pt–Sn alloys, opening the road for an improved understanding of electro-oxidation and catalysis of alcohols and other oxygenated molecules on bimetallic Pt–Sn catalysts.

References

[1] C. Lamy, Electrochim. Acta. 29 (1984) 1581.
[2] S. Surampudi, S.R. Narayanan, E. Vamos, H. Frank, G. Halpert, A. La Conti, J. Kosek, G.K. Surya Prakash, G.A. Olah, J. Power Sources 47 (1994) 377.
[3] E.M. Belgsir, H. Huser, J.M. Leger, C. Lamy, J. Electroanalyt. Chem. 225 (1987) 281.
[4] F. Kadirgam, B. Beden, J.M. Leger, C. Lamy, J. Electroanalyt. Chem. 125 (1981) 89.
[5] M. Shibata, S. Motoo, J. Electroanalyt. Chem. 209 (1996) 151.
[6] K. Kunimatsu, J. Electroanalyt. Chem. 213 (1986) 149.
[7] P. Olivi, B. Beden, F. Hahn, J.M. Leger, C. Lamy, J. Electroanalyt. Chem. 346 (1993) 415.
[8] B. Beden, S. Juanto, J.M. Leger, C. Lamy, J. Electroanalyt. Chem. 238 (1987) 323.
[9] T. Iwasita, W. Vielstich, E. Santos, J. Electroanalyt. Chem. 229 (1987) 367.
[10] R. Parsons, T. Vandernoot, J. Electroanalyt. Chem. 257 (1988) 9.
[11] R. Adzic, in: H. Gerischer (Ed.), Advances in Electrochemistry and Electrochemistry Engineering, vol 13, Wiley, New York, 1984, pp. 159–260.
[12] M.M.P. Janssen, J. Moolhuysen, Electrochim. Acta. 21 (1976) 869.
[13] M.M.P. Janssen, J. Moolhuysen, Electrochim. Acta. 21 (1976) 861; J. Catal. 46 (1977) 289.
[14] K. Wang, H.A. Gasteiger, N.M. Markovic, P.N. Ross, Jr., Electochim. Acta. 41 (1996) 2587.
[15] K.J. Cathro, J. Electrochem. Soc. 116 (1969) 1608.
[16] S. Szabo, J. Electroanalyt. Chem. 172 (1984) 359.
[17] S. Gilman, M.W. Breiter, J. Electrochem. Soc. 109 (1962) 1099.
[18] A.N. Haner, P.N. Ross, J. Phys. Chem. 95 (1991) 3740.
[19] S.A. Campbell, R. Parsons, J. Chem. Soc. Faraday Trans. 88 (6) (1992) 833.
[20] J. Willsam, J. Heitbaum, Electrochim. Acta. 31 (1986) 943.
[21] B. Beden, M.C. Morin, F. Hahn, C. Lamy, J. Electroanalyt. Chem. 229 (1987) 353.
[22] J.L. Davis, M.A. Barteau, Surf. Sci. 187 (1987) 387.
[23] S. Akhter, J.M. White, Surf. Sci. 167 (1986) 101.
[24] J. Wang, R.I. Masel, Surf. Sci. 243 (1991) 199.
[25] B.A. Sexton, K.D. Rendulic, A.E. Hughes, Surf. Sci. 121 (1982) 181.
[26] K.D. Gibson, L.H. Dubois, Surf. Sci. 223 (1990) 59.
[27] P.A. Thiel, T.E. Madey, Surf. Sci. Rep. 7 (1987) 211.
[28] G.B. Fisher, J.L. Gland, Surf. Sci. 94 (1980) 446.
[29] S.K. Jo, J. Kiss, J.A. Polanco, J.M. White, Surf. Sci. 253 (1991) 233.
[30] E. Langenbach, A. Spitzer, H. Luth, Surf. Sci. 147 (1984) 179.
[31] H. Ibach, S. Lehwald, Surf. Sci. 91 (1980) 187.
[32] F.T. Wagner, T.E. Moylan, Surf. Sci. 191 (1987) 121.
[33] M.T. Paffett, R.G. Windham, Surf. Sci. 208 (1989) 34.
[34] S.H. Overbury, D.R. Mullins, M.T. Paffett, B.E. Koel, Surf. Sci. 254 (1991) 45.

[35] L.Q. Jiang, B.E. Koel, J. Phys. Chem. 96 (1992) 8694.
[36] C. Xu, B.E. Koel, J. Chem. Phys. 100 (1994) 664.
[37] P.A. Redhead, Vacuum 12 (1962) 203.
[38] J.B. Miller, H.R. Siddiqui, S.M. Gates, J.N. Russell, J.T. Yates, Jr., J.C. Tully, J.M. Cardillo, J. Chem. Phys. 87 (1987) 6725.
[39] D.H. Parker, M.E. Jones, B.E. Koel, Surf. Sci. 233 (1990) 65.
[40] C. Xu, B.E. Koel, Surf. Sci. 304 (1994) L505.
[41] M.T. Paffett, S.C. Gebhard, R.G. Windham, B.E. Koel, J. Phys. Chem. 94 (1990) 6831.
[42] Y.-L. Tsai, C. Xu, B.E. Koel, Surf. Sci. 385 (1997) 37.